

Supplementary Material for

Microbial and geochemical evidence of permafrost formation at Mamontova Gora and Syrdakh, Central Yakutia

Cherbunina M.Yu.^{1*}, Karaevskaya E.S.², Vasil'chuk Yu.K.³, Tananaev N.I.⁴, Shmelev D.G.¹ Budantseva N.A.³, Merkel A.Yu⁵, Rakitin A.I.⁶, Mardanov A.V.⁶, Brouchkov A. V.¹, Bulat S.A.^{7,8}

¹ Lomonosov Moscow State University, Faculty of Geology, Moscow, Russia

² Arctic and Antarctic Research Institute (AARI), St. Petersburg, Russia

³ Lomonosov Moscow State University, Faculty of Geography, Moscow, Russia

⁴ The Melnikov Permafrost Institute, Siberian Branch of the Russian Academy of Sciences, Yakutsk, Russia

⁵ Winogradsky Institute of Microbiology, Research Center of Biotechnology, Russian Academy of Sciences, Moscow, Russia

⁶ Institute of Bioengineering, Research Center of Biotechnology, Russian Academy of Sciences, Moscow, Russia

⁷ Petersburg Nuclear Physics Institute named by B.P. Konstantinov of NRC “Kurchatov Institute”, Gatchina, Russia

⁸ Institute of Physics and Technology, Ural Federal University, Ekaterinburg, Russia

Supplementary figures

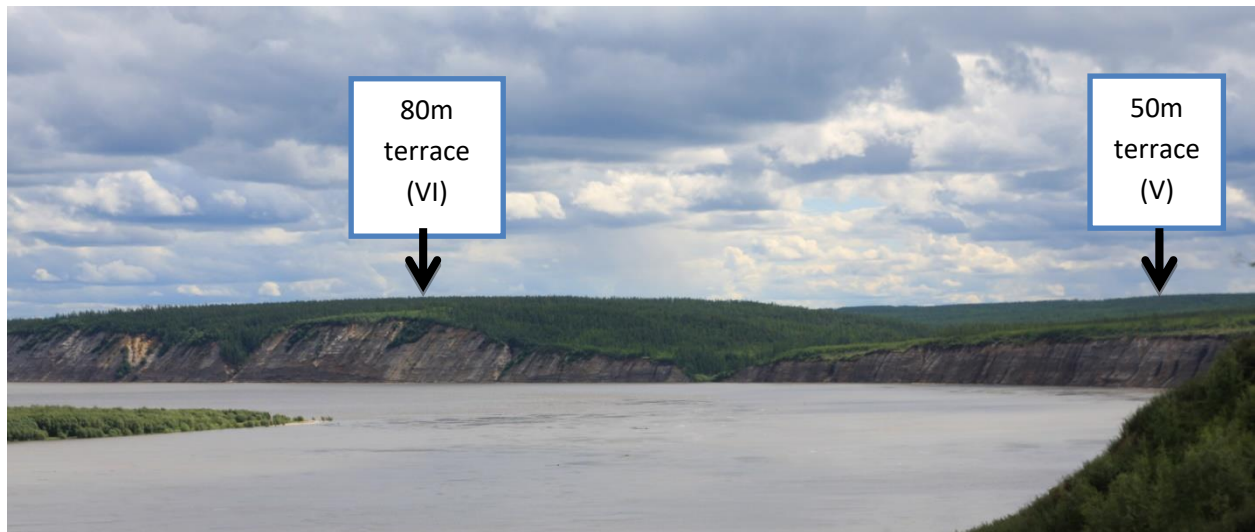


Figure S1. V and VI terraces of the Aldan River (photo by Vladimir Karzhavin)



Figure S2. Mamontova Gora.Thawing of the IC of the 50-meter terrace (V) of Aldan River (photo by D. Shmelev)

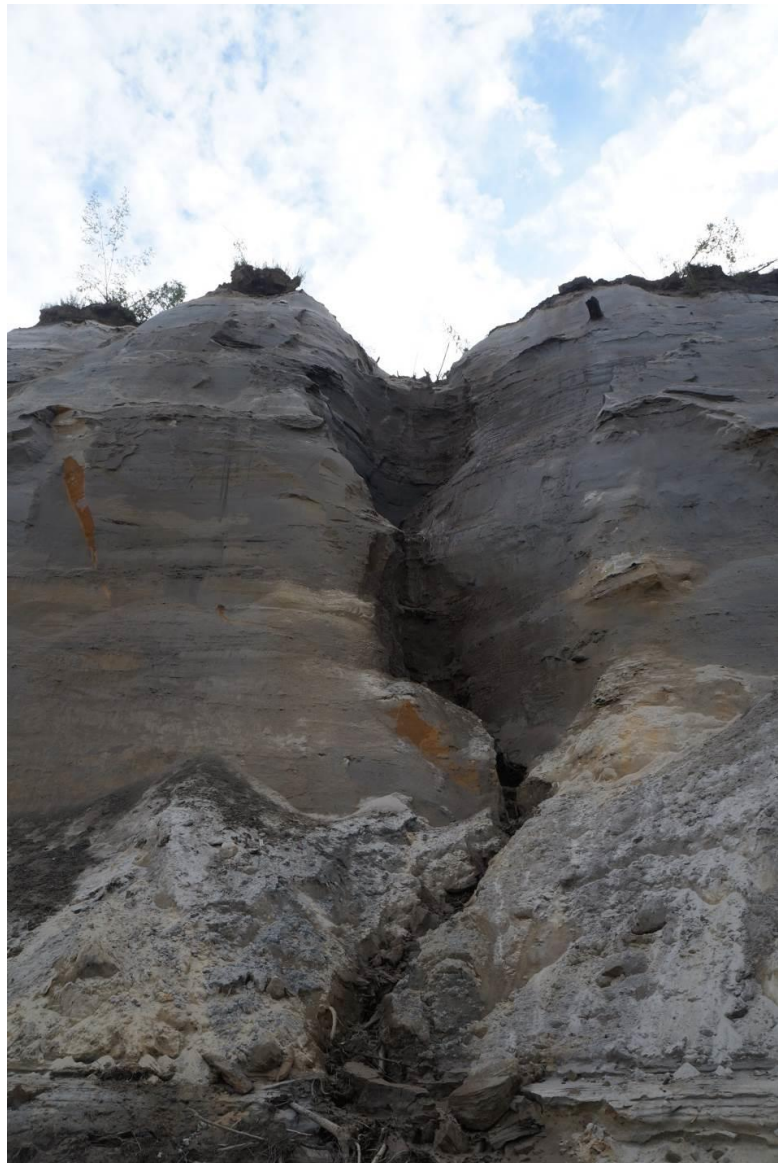


Figure S3. Thick ice wedges of the V terrace of Mamontova gora IC (two horizons) (photo by M. Cherbunina)



Figure S4. Holocene (modern) ice wedges of the modern floodplain of the right bank of Aldan River in different sections: a) longitudinal and b) transverse section (photo by V. Karzhavin).)

a)



b)



Figure S5. Forming slope washes at the foot of the Neogene-Middle Pleistocene strata due to thawing of the overlying IC (a) and a fragment of a layered aluvial sand (b) (photo by D.G. Shmelev

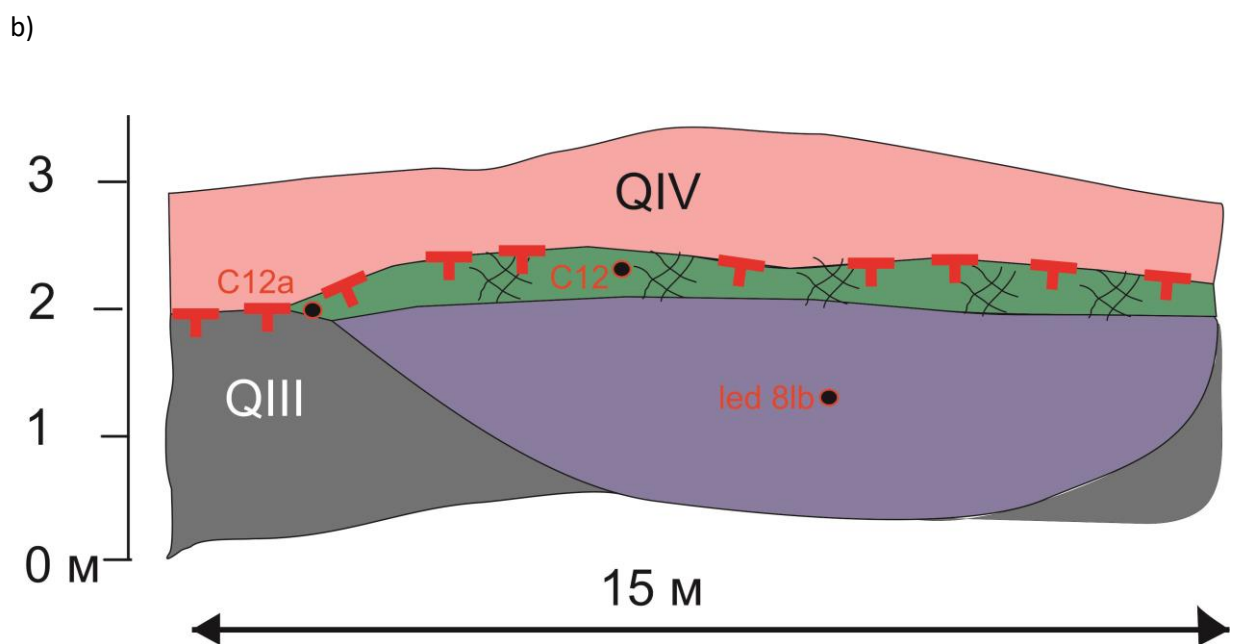
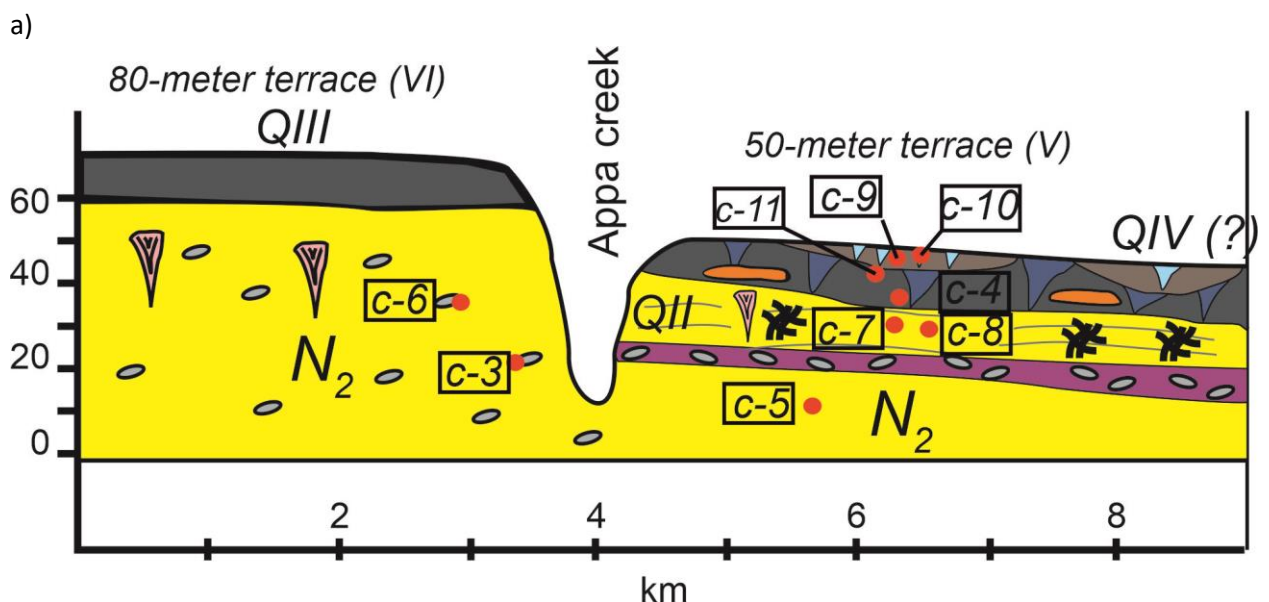


Figure S6. Sampling points for further profiling of prokaryotic communities based on 16S rRNA gene a) Mamontova gora b) Syrdakh

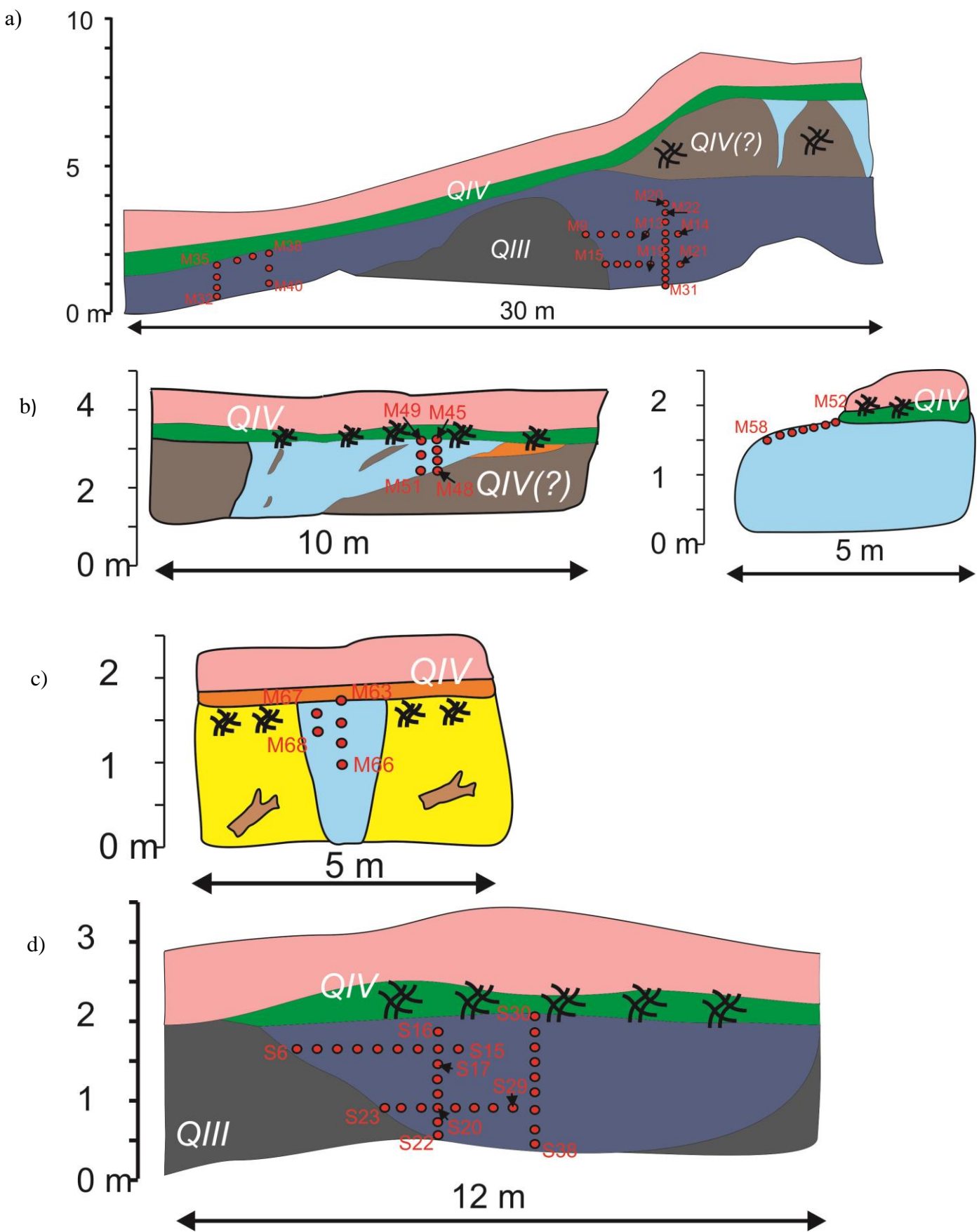


Figure S7. Sampling points for isotopic analysis of underground ice from the outcrops of Mamontova Gora, Syrdakh and the modern floodplain. a) The lower horizon of the Mamontova Gora IC b) The upper horizon of the Mamontova Gora IC c) modern floodplain ice d) Syrdakh IC. For other symbols see legend for Figure 2 in the text.

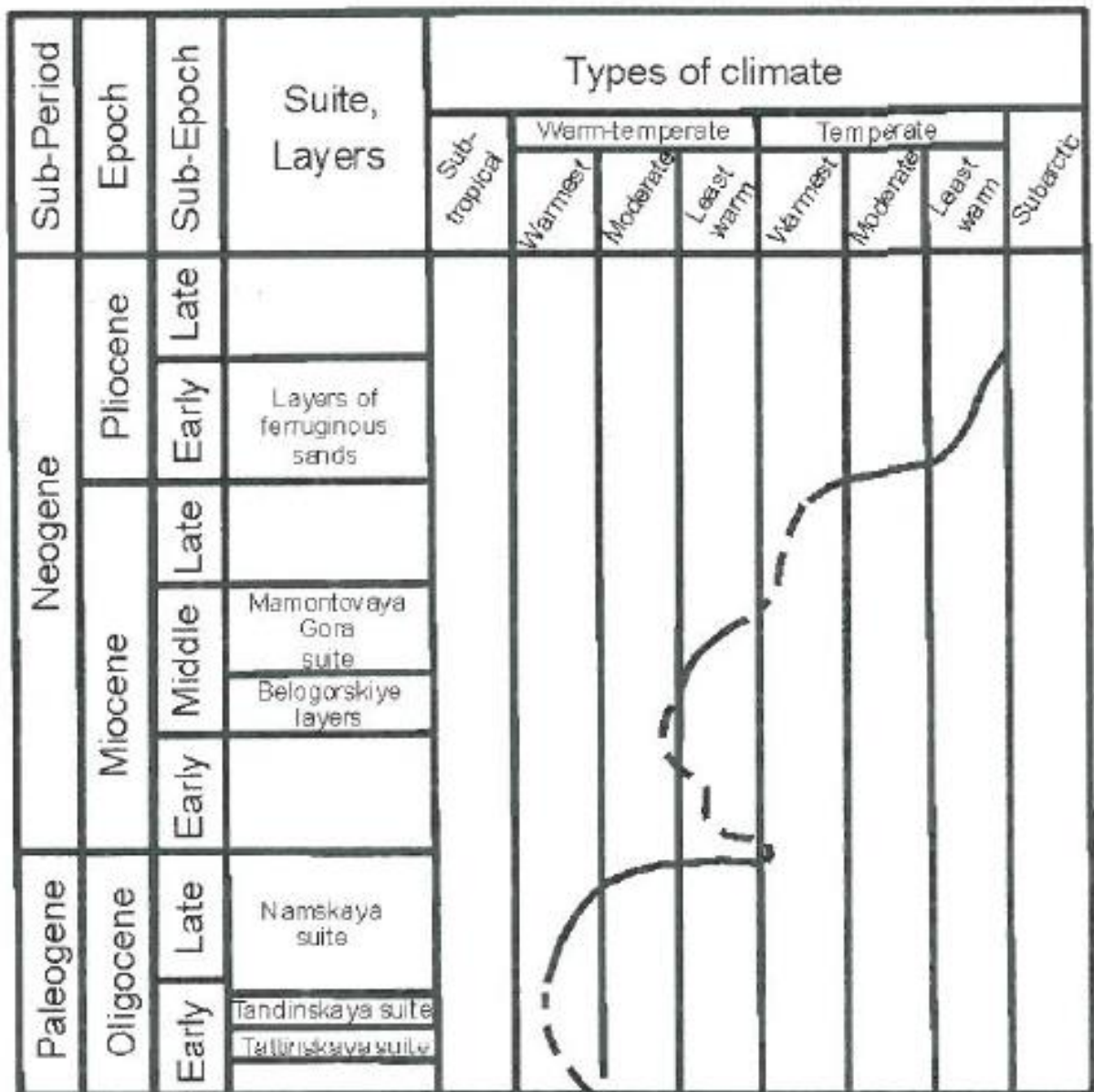


Figure S8. The dynamics of the landscape-climatic conditions in Oligocene-Pliocene according to Fradkina et al, 2005

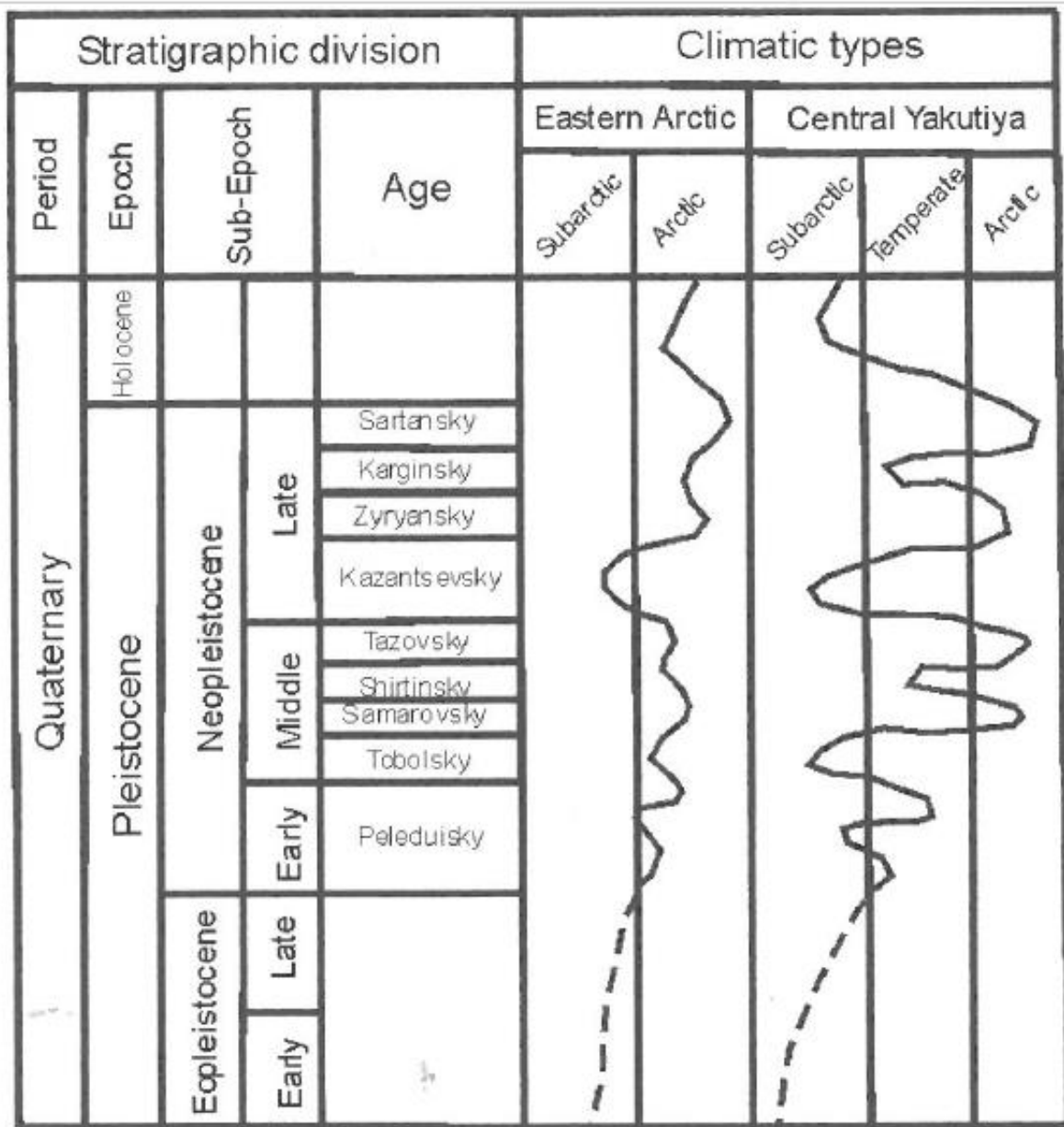


Figure S9 Dynamics of quaternary dynamics conditions of the Eastern arctic according to Fradkina et al, 2005.

Supplementary tables

Table 1. Results of radiocarbon dating of the Mamontova Gora sample (peat loam containing veins of the upper horizon, sampling depth 2.1 m) and Syrdakh (the loam located directly above the ice wedge).

Nº	IGAN AMS	UGAMS	Sample	Mat erial	^{14}C , BP (1 σ)	pMC	cal BP
1	5490	29045	Mamon tova gora	TC	39590±300	0.724±0.026	68.3 (1 sigma) cal BP 42974 - 43516 1.000 95.4 (2 sigma) cal BP 42760 - 43884 1.000 Median Probability: 43268
2	5491	29046	Syrdakh	TC	9430±30	30,929±0.026	68.3 (1 sigma) cal BP 10594 - 10625 0.332 10649 - 10704 0.668 95.4 (2 sigma) cal BP 10580 - 10735 1.000 Median Probability: 10662

Reference

RADIOCARBON CALIBRATION PROGRAM CALIB REV7.1.0 Copyright 1986-2016 M Stuiver and PJ Reimer Reimer, P., Bard, E., Bayliss, A., Beck, J., Blackwell, P., Ramsey, C., . . . Van der Plicht, J. (2013). IntCal13 and Marine13 Radiocarbon Age Calibration Curves 0–50,000 Years cal BP. Radiocarbon, 55(4), 1869-1887. doi:10.2458/azu_js_rc.55.16947

Table 2. Bray–Curtis dissimilarity values calculated for 16S rRNA gene sequence data at phylum level

	C3	C6	C5	C4	C7	C8	C11	C10	C9	C12	C12a	ledS	AL	MMG	MMP
C3	0.00	0.15	0.26	0.47	0.43	0.57	0.56	0.55	0.76	0.78	0.61	0.65	0.63	0.67	0.56
C6	0.15	0.00	0.32	0.43	0.39	0.53	0.53	0.54	0.71	0.77	0.68	0.66	0.61	0.61	0.48
C5	0.26	0.32	0.00	0.38	0.64	0.78	0.52	0.46	0.68	0.58	0.49	0.54	0.53	0.55	0.62
C4	0.47	0.43	0.38	0.00	0.38	0.52	0.22	0.27	0.42	0.56	0.42	0.25	0.50	0.39	0.34
C7	0.43	0.39	0.64	0.38	0.00	0.14	0.38	0.63	0.62	0.89	0.74	0.56	0.74	0.73	0.29
C8	0.57	0.53	0.78	0.52	0.14	0.00	0.37	0.70	0.62	0.89	0.78	0.58	0.75	0.74	0.31
C11	0.56	0.53	0.52	0.22	0.38	0.37	0.00	0.33	0.32	0.58	0.45	0.28	0.50	0.46	0.26
C10	0.55	0.54	0.46	0.27	0.63	0.70	0.33	0.00	0.45	0.42	0.27	0.30	0.45	0.32	0.58
C9	0.76	0.71	0.68	0.42	0.62	0.62	0.32	0.45	0.00	0.29	0.47	0.25	0.58	0.54	0.57
C12	0.78	0.77	0.58	0.56	0.89	0.89	0.58	0.42	0.29	0.00	0.29	0.40	0.45	0.48	0.84
C12a	0.61	0.68	0.49	0.42	0.74	0.78	0.45	0.27	0.47	0.29	0.00	0.30	0.46	0.41	0.70
ledS	0.65	0.66	0.54	0.25	0.56	0.58	0.28	0.30	0.25	0.40	0.30	0.00	0.59	0.40	0.52
AL	0.63	0.61	0.53	0.50	0.74	0.75	0.50	0.45	0.58	0.45	0.46	0.59	0.00	0.29	0.69
MMG	0.67	0.61	0.55	0.39	0.73	0.74	0.46	0.32	0.54	0.48	0.41	0.40	0.29	0.00	0.68
MMP	0.56	0.48	0.62	0.34	0.29	0.31	0.26	0.58	0.57	0.84	0.70	0.52	0.69	0.68	0.00

Table 3 . Bray–Curtis dissimilarity values calculated for 16S rRNA gene sequence data at class level

	c3	c6	c5	c4	c7	c8	c11	c10	c9	c12	c12a	led8	AL	MMG	MMP
c3	0.00	0.19	0.38	0.57	0.46	0.56	0.58	0.63	0.81	0.86	0.67	0.74	0.69	0.68	0.85
c6	0.19	0.00	0.44	0.57	0.49	0.60	0.52	0.59	0.71	0.79	0.67	0.69	0.69	0.64	0.77
c5	0.38	0.44	0.00	0.61	0.74	0.81	0.66	0.69	0.78	0.72	0.64	0.75	0.64	0.73	0.80
c4	0.57	0.57	0.61	0.00	0.44	0.53	0.42	0.33	0.62	0.79	0.67	0.58	0.56	0.45	0.61
c7	0.46	0.49	0.74	0.44	0.00	0.15	0.64	0.69	0.77	0.87	0.74	0.77	0.80	0.78	0.59
c8	0.56	0.60	0.81	0.53	0.15	0.00	0.68	0.76	0.77	0.88	0.81	0.83	0.82	0.80	0.47
c11	0.58	0.52	0.66	0.42	0.64	0.68	0.00	0.39	0.44	0.70	0.61	0.35	0.62	0.56	0.68
c10	0.63	0.59	0.69	0.33	0.69	0.76	0.39	0.00	0.49	0.54	0.51	0.42	0.54	0.41	0.80
c9	0.81	0.71	0.78	0.62	0.77	0.77	0.44	0.49	0.00	0.41	0.50	0.41	0.71	0.72	0.68
c12	0.86	0.79	0.72	0.79	0.87	0.88	0.70	0.54	0.41	0.00	0.38	0.59	0.64	0.77	0.92
c12a	0.67	0.67	0.64	0.67	0.74	0.81	0.61	0.51	0.50	0.38	0.00	0.55	0.65	0.73	0.90
led8	0.74	0.69	0.75	0.58	0.77	0.83	0.35	0.42	0.41	0.59	0.55	0.00	0.72	0.64	0.77
AL	0.69	0.69	0.64	0.56	0.80	0.82	0.62	0.54	0.71	0.64	0.65	0.72	0.00	0.41	0.90
MMG	0.68	0.64	0.73	0.45	0.78	0.80	0.56	0.41	0.72	0.77	0.73	0.64	0.41	0.00	0.85
MMP	0.85	0.77	0.80	0.61	0.59	0.47	0.68	0.80	0.68	0.92	0.90	0.77	0.90	0.85	0.00